Calculation of Three-Dimensional Boundary Layers: III. Three-Dimensional Flows in Orthogonal Curvilinear Coordinates

Tuncer Cebeci,* Kalle Kaups,† and Alfred Moser‡
Douglas Aircraft Company, Long Beach, Calif.

This paper describes a general method for solving the three-dimensional laminar and turbulent boundary-layer equations in orthogonal curvilinear coordinates. As in the earlier two papers, the Reynolds shear-stress terms are modeled by an eddy viscosity formulation developed by Cebeci and the governing equations are solved by a very efficient two-point finite-difference method. The accuracy of the method is investigated for turbulent flows.

Nomenclature

A	= Van Driest damping parameter, see Eq. (15b)
c_{f_s}	= local skin-friction coefficient in streamwise direction
f	= transformed vector potential for ψ
g	= transformed vector potential for Φ
h_1, h_2	= metric coefficients
H	= boundary-layer shape factor, see Eq. (28)
K_1, K_2	= geodesic curvatures of coordinate lines
L	= modified mixing length, see Eq. (15a)
p	= static pressure
P_i	= coefficients in the transformed momentum equations, see Eq. (12b)
q	= velocity vector parallel to surface
$\bar{q}$	= magnitude of velocity vector
q_e	= magnitude of velocity vector at boundary-layer edge
R_s	= Reynolds number $u_e s_1/\nu$
R_θ	= momentum thickness Reynolds number, see Eq. (28)
s_1	= arc length along x-coordinate
$R_{\delta_1^*}$	= displacement thickness Reynolds number
S	= shear vector $\partial q/\partial y$
u, v, w	= velocity components in the x, y, z directions
u_τ	= friction velocity
x	= curvilinear surface coordinate
y	= distance normal to the body surface
z	= curvilinear surface coordinate orthogonal to the x coordinate
β	= cross-flow angle relative to inviscid flow direction
δ	= boundary-layer thickness
ϵ	= eddy viscosity
ϵ^+	= dimensionless eddy viscosity, ϵ/ν
η	= similarity variable, see Eq. (5)
μ	= dynamic viscosity
ν	= kinematic viscosity
ρ	= density
τ	= shear stress
ϕ, ψ	= two-component vector potential, see Eq. (7)

Subscripts

e	= boundary-layer edge
s	= streamwise direction
w	= wall
$(\ )'$	= differentiation with respect to η

Received Oct. 7, 1975; revision received April 8, 1976. This work was supported by the Naval Ship Research and Development Center under contract N00014-72-C-0111, sub project SR 009 01-01.

Index category: Boundary Layers and Convective Heat Transfer—Turbulent.

*Chief Aerodynamics Engineer, Research. Member AIAA.
†Senior Engineer/Scientist. Member AIAA.
‡Engineer Scientist Specialist. Member AIAA.

I. Introduction

In Ref. 1, Cebeci described a general method for solving the laminar and turbulent boundary-layer equations for swept infinite cylinders and for small cross flows. In the equations, the Reynolds shear stress terms were modeled by using an eddy-viscosity concept. A very efficient and accurate two-point finite-difference method was used to solve the governing equations. The accuracy of the method was investigated for several flows by comparing the calculated results with experiment and with those obtained by Bradshaw.[2] In general, the agreement with experiment and with Bradshaw's results were quite satisfactory. In Ref. 3, Cebeci extended the method to three-dimensional flows in Cartesian coordinates, and again obtained good agreement with experiment. In the present paper, the authors extend the method to three-dimensional flows in orthogonal coordinates, and present a comparison of several calculated results with experiment.

II. Boundary-Layer Equations

The governing boundary-layer equations for three-dimensional incompressible flows in a curvilinear orthogonal coordinate system are given by the following equations:

Continuity

$$(\partial/\partial x)(h_2 u) + (\partial/\partial z)(h_1 w) + (\partial/\partial y)(h_1 h_2 v) = 0 \tag{1}$$

x-momentum

$$\frac{u}{h_1}\frac{\partial u}{\partial x} + \frac{w}{h_2}\frac{\partial u}{\partial z} + v\frac{\partial u}{\partial y} - uwK_1 + w^2 K_2 = -\frac{1}{\rho h_1}\frac{\partial p}{\partial x} + \frac{\partial}{\partial y}\left(\nu\frac{\partial u}{\partial y} - \overline{u'v'}\right) \tag{2}$$

z-momentum

$$\frac{u}{h_1}\frac{\partial w}{\partial x} + \frac{w}{h_2}\frac{\partial w}{\partial z} + v\frac{\partial w}{\partial y} - uwK_2 + u^2 K_1 = -\frac{1}{\rho h_2}\frac{\partial p}{\partial z} + \frac{\partial}{\partial y}\left(\nu\frac{\partial w}{\partial y} - \overline{w'v'}\right) \tag{3}$$

Here h_1 and h_2 are metric coefficients and are functions of x and z, and the parameters K_1 and K_2 are known as the geodesic curvatures of the curves $z=$ const and $x=$ const, respectively.

The boundary conditions for Eqs. (1-3) for zero mass transfer are

$$y=0 \qquad u,w,v=0 \tag{4}$$

$$y\to\infty \qquad u\to u_e(x,z) \qquad w\to w_e(x,z)$$

Before we solve the previous system, we first transform it. We define the transformed coordinates by

$$x=x \qquad z=z \qquad \eta=(u_e/\nu s_1)^{1/2}y \tag{5}$$

and introduce a two-component vector potential such that

$$h_2u=\frac{\partial\psi}{\partial y} \qquad h_1w=\frac{\partial\phi}{\partial y} \qquad h_1h_2v=-\left(\frac{\partial\psi}{\partial x}+\frac{\partial\phi}{\partial z}\right) \tag{6}$$

In addition, the dimensionless variables f and g related to ψ and ϕ are defined by

$$\psi=(u_e\nu s_1)^{1/2}h_2f(x,z,\eta) \tag{7a}$$

$$\phi=(u_e\nu s_1)^{1/2}h_1(w_e/u_e)g(x,z,\eta) \tag{7b}$$

Here s_1, which denotes the arc length along the x coordinate, is defined by

$$s_1=\int_0^x h_1dx \tag{8}$$

With the concept of eddy viscosity and with the previous transformed variables, it can be shown that the system of Eqs. (1-4) can be written as

x-momentum equation

$$(bf'')'+P_1ff''+P_2[1-(f')^2]+P_5[1-f'g'] +P_6f''g+P_8[1-(g')^2] =xP_{10}\left[f'\frac{\partial f'}{\partial x}-f''\frac{\partial f}{\partial x}+P_7\left(g'\frac{\partial f'}{\partial z}-f''\frac{\partial g}{\partial z}\right)\right] \tag{9}$$

z-momentum equation

$$(bg'')'+P_1fg''+P_4(1-f'g')+P_3[1-(g')^2] +P_6gg''+P_9[1-(f')^2] =xP_{10}\left[f'\frac{\partial g'}{\partial x}-g''\frac{\partial f}{\partial x}+P_7\left(g'\frac{\partial g'}{\partial z}-g''\frac{\partial g}{\partial z}\right)\right] \tag{10}$$

$$\eta=0 \qquad f=g=f'=g'=0 \tag{11a}$$

$$\eta=\eta_\infty \qquad f'=g'=1 \tag{11b}$$

Here the primes denote differentiation with respect to η, and

$$b=1+\epsilon^+ \qquad \epsilon^+=\epsilon/\nu \qquad f'=u/u_e \qquad g'=w/w_e \tag{12a}$$

The coefficients P_1 and P_{10} are functions of u_e, w_e, h_1, h_2, K_1, and K_2, and are given by the following formulas:

$$P_1=(M+1)/2-s_1K_2 \qquad P_2=M \qquad P_3=R$$

$$P_4=\left(\frac{u_e}{w_e}\right)Q-s_1K_2 \qquad P_5=\frac{w_e}{u_e}(N-s_1K_1)$$

$$P_6=R+\frac{w_e}{2u_e}\left(\frac{1}{h_1}\frac{\partial s_1}{\partial z}-N\right)-\left(\frac{w_e}{u_e}\right)s_1K_1$$

$$P_7=\frac{h_1}{h_2}\frac{w_e}{u_e} \qquad P_8=\left(\frac{w_e}{u_e}\right)^2s_1K_2$$

$$P_9=\left(\frac{u_e}{w_e}\right)s_1K_1 \qquad P_{10}=\frac{s_1}{x} \tag{12b}$$

$$M=\frac{s_1}{u_eh_1}\frac{\partial u_e}{\partial x} \qquad N=\frac{s_1}{u_eh_2}\frac{\partial u_e}{\partial z}$$

$$Q=\frac{s_1}{u_eh_1}\frac{\partial w_e}{\partial x} \qquad R=\frac{s_1}{u_eh_2}\frac{\partial w_e}{\partial z}$$

III. Eddy-Viscosity Formulation

The authors use the eddy-viscosity formulation of Refs. 1 and 3, and define ϵ by two separate formulas. With the definition of the velocity vector parallel to the wall, $q=(u, w)$ and the shear or strain vector $S=\partial q/\partial y=(\partial u/\partial y, \partial w/\partial y)$, the eddy viscosity formulas for the inner and outer regions are

$$\epsilon=\begin{cases}\epsilon_i=L^2|S(y)| & \epsilon_i\leq\epsilon_0 \quad (13)\\ \epsilon_0=0.0168\int_0^\infty(|q_e|-|q(y)|)dy & \epsilon_i\geq\epsilon_0 \quad (14)\end{cases}$$

Here

$$L=0.4y[1-\exp(-y/A)] \tag{15a}$$

$$A=26(\nu/|S_w|)^{1/2} \tag{15b}$$

IV. Comparison with Experiment

Calculation for a Curved Rectangular Duct

In order to test the present method, we have considered two test cases. The first one deals with the boundary layer on one of the two plane walls in a 60° curved duct of rectangular cross section. Figure 1 shows a sketch of the flow geometry. The experimental data are due to Vermeulen.[4] Here z denotes the distance from the outer wall, measured along normals to that wall; x denotes the arc length along the outer wall; and y denotes distance normal to the plane x, z.

The solution of the three-dimensional boundary-layer equations requires initial conditions on two intersecting planes. These initial conditions can be obtained in a number of ways; here they are obtained from experiment. For the investigated curved duct, the streamlines within the boundary layer generally turn more sharply than the edge streamlines, because of the need to balance the radial (z-direction) static pressure gradient. The measured limiting streamlines, that is, the curves to which the wall shear vectors are tangential, also show this (see Fig. 2). "Information" within the boundary layer is carried from the outer curved wall inward, as well as from the inlet cross-section downstream. For this reason, we have chosen to start the calculations from the upstream and outer edges of the bend. The procedure described in the following was used to generate the initial velocity profiles.

According to Coles' velocity profile formula (see, for example, Ref. 5)

$$u^+=\Phi(y^+)+(2\Pi/\kappa)\sin^2[(\pi/2)/(y/\delta)] \tag{16}$$

Here $\kappa=0.41$, $u^+=u/u_\tau, u_\tau=(\tau_w/\rho)^{1/2}$, and $\Phi(y^+)$ is given by

$$\Phi(y^+)=\int_0^{y^+}\frac{2dy^+}{1+\{1+4(ky^+)^2[1-\exp(-y^+/24.4)]^2\}^{1/2}} \tag{17}$$

with $y^+=yu_\tau/\nu$.

Equation (16) represents the experimental data rather well for two-dimensional flows. Here, as in Ref. 1, the authors use

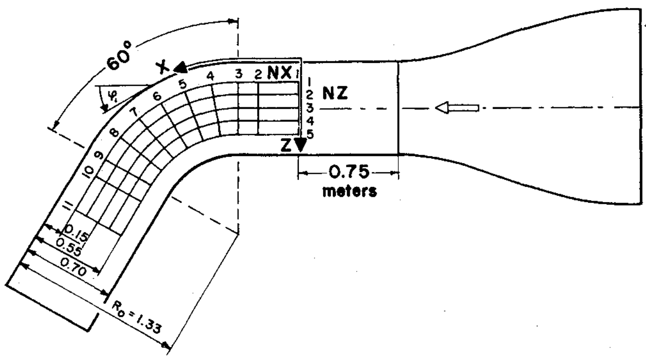

Fig. 1 Flow geometry for the curved rectangular duct.

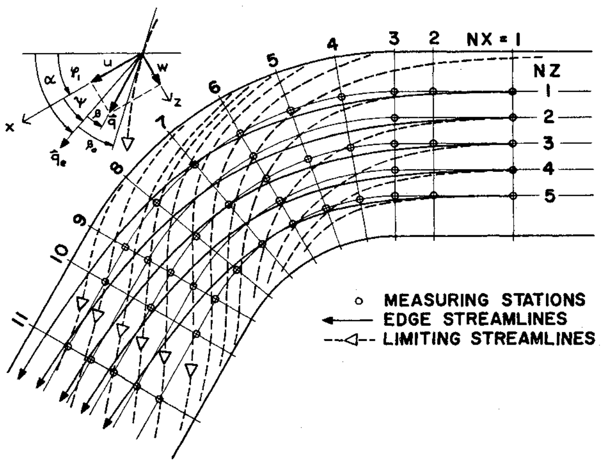

Fig. 2 Experimental streamlines measured by Vermeulen.[4]

it to compute three-dimensional flows by assuming it to apply to the streamwise velocity profile, but replacing u^+ by q_s^+, where

$$q_s^+ = q_s/u_\tau \qquad u_\tau = (\tau_{w_s}/\rho)^{1/2} \tag{18}$$

In terms of streamwise skin-friction coefficient c_{f_s}, the friction velocity u_τ can be written as

$$u_\tau = q_e(c_{f_s}/2)^{1/2} \tag{19}$$

In order to generate the streamwise velocity profile from Eq. (16), the authors use the initial values of c_{f_s} and $R_{\delta_1^*}$, and determine the dimensionless boundary-layer thickness δ^+ and the profile parameter Π from the following expressions:

$$\delta^+ = \exp\{[(2/c_{f_s})^{1/2} - 5.0 + 2/\kappa - 2R_{\delta_1^*}/\delta^+]\kappa\} \tag{20}$$

$$\Pi = (R_{\delta_1^*}/\delta^+)\kappa - 1 \tag{21}$$

In order to generate the cross-flow velocity component q_n, Mager's expression is used, and q_n is defined by

$$q_n = q_s \tan\beta_w (1 - y/\delta)^2 \tag{22}$$

with the wall cross flow angle β_w obtained from the experimental data.

Once the streamwise and cross-flow velocity profiles are calculated by the above procedure we calculate the velocity profiles u/u_e and w/w_e in the orthogonal directions x and z by the following relationships:

$$u/u_e = q_s/q_e - (q_n/q_e)(w_e/u_e) \tag{23}$$

$$w/w_e = q_s/q_e + (q_n/q_e)(u_e/w_e) \tag{24}$$

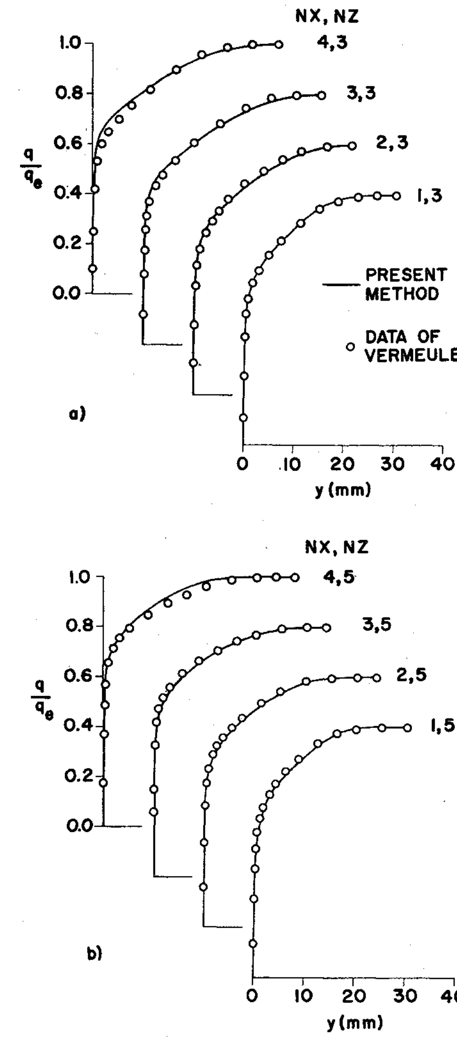

Fig. 3 Comparison of calculated and experimental velocity profiles for the data of Vermeulen at: a) $z(3) = 0.35$ m, and b) $z(5) = 0.55$ m.

The solution of the governing equations also requires the specification of the metric coefficients and the geodesic curvatures. They are calculated from the following expressions:

$$h_1 = \frac{\partial s_1}{\partial x} = \begin{cases} 1 & \text{straight section} \\ 1 - z/R_0 & \text{curved section} \end{cases}$$

$$h_2 = \frac{\partial s_2}{\partial z} = 1.0$$

$$K_1 = \frac{\partial \phi_1}{\partial s_1} = \begin{cases} 0 & \text{straight section} \\ 1/(R_0 - z) & \text{curved section} \end{cases}$$

$$K_2 = \partial\phi_2/\partial s_2 = 0$$

Here s_1 and s_2 are lengths and ϕ_1 and ϕ_2 are directional angles of the x and z coordinates, respectively; ($d\phi_1$ is positive for rotation in the $+z$ direction). Note that h_1 and K_1 have discontinuities at both ends of the curved section, but both s and ϕ are continuous.

A comparison of calculated and experimental results is shown in Figs. 3 and 4. Figure 3 shows the dimensionless resultant velocity ratio q/q_e along the lines $z(3) = 0.35$ m and

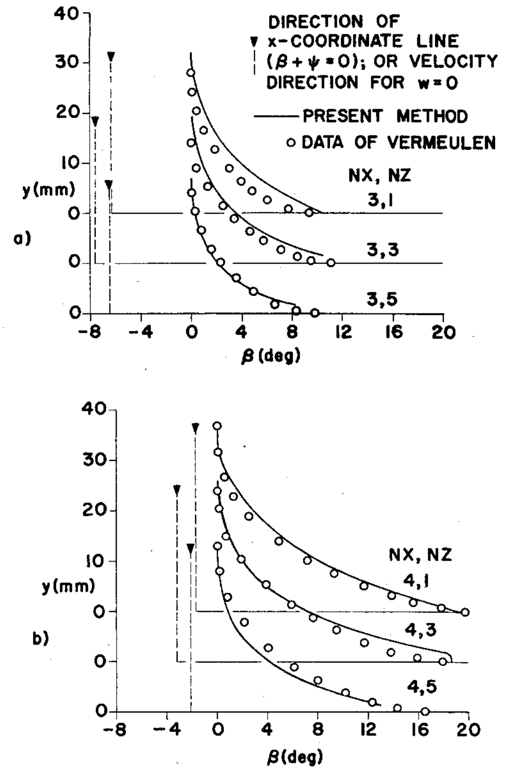

Fig. 4 Comparison of calculated and experimental cross-flow angle β between velocity vector and edge streamline: a) $NX=3$, b) $NX=4$.

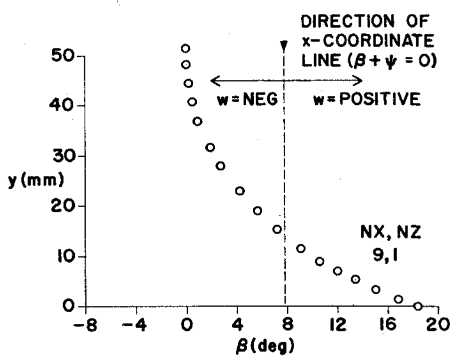

Fig. 5 Experimental profile of cross-flow angle indicating layers of positive and negative values of the z-velocity component w.

$z(5)=0.55$ m. Here

$$\frac{q}{q_e}=\left[\frac{(f')^2+(w_e/u_e g')^2}{1+(w_e/u_e)^2}\right] \tag{25}$$

Figure 4 shows the cross flow angle β distribution across the boundary layer for several stations; β is defined by

$$\sin\beta=\frac{-w_e u+u_e w}{qq_e}=\frac{w_e/u_e(g'-f')}{(q/q_e)(q_e/u_e)^2} \tag{26}$$

At the wall

$$\tan\beta=\frac{w_e/u_e(g''_w-f''_w)}{(w_e/u_e)^2 g''_w+f''_w} \tag{27}$$

The method in its present form is unable to compute boundary layers such as those measured at station $NX=9$, $NZ=1$ (see Fig. 5). At this station, for example, the direction of the velocity vector with respect to the x coordinate varies between

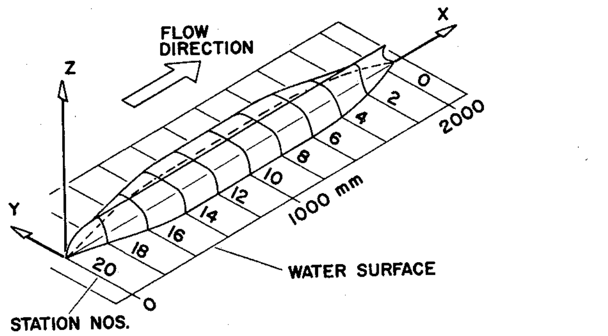

Fig. 6 Hull model of cargo liner, SSPA model 720, tested by Larsson.[6] Actual model consists of two shapes, as shown, to produce plane of symmetry at load waterline.

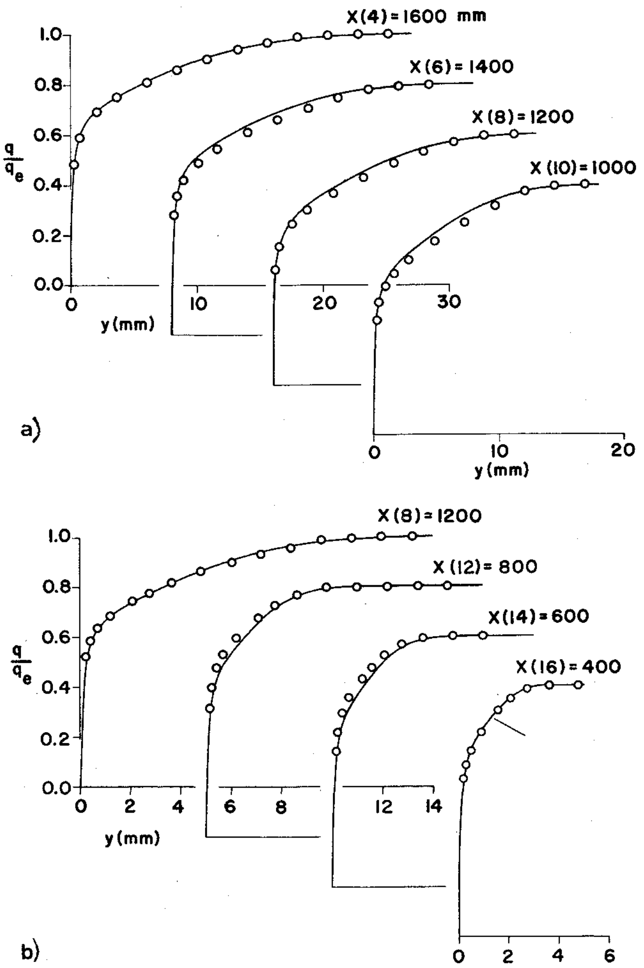

Fig. 7 Comparison of calculated and experimental velocity profiles for the data of Larsson.[6] a) For streamline no. 3. b) For streamline no. 5

$(\psi+\beta)=+10°$ at the surface and $(\psi+\beta)=-8°$ at the edge of the boundary layer. This problem, called "inflow," can be avoided by selecting a coordinate system in which the boundary-layer velocity vectors remain between the positive x and z coordinate directions for all stations $\{$i.e., $0<[\psi+\beta(y)]<\pi/2\}$. It also may be avoided by changing the present finite-difference molecule. Obviously, further studies are required in this area.

Calculations for a Cargo-Ship Model

The second test case deals with the comparison of calculated and experimental results for three-dimensional turbulent boundary layers on the model of a cargo ship. The experimental data are due to Larsson.[6] The model of 2.0-m

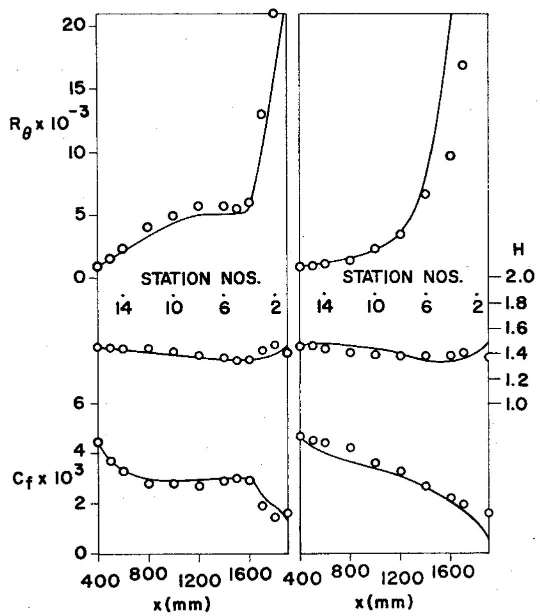

Fig. 8 Comparison of calculated and experimental results for the data of Larsson[6]: left-hand side-streamline no. 3; right-hand side—streamline no. 5.

length was tested in the low-speed wind tunnel at Chalmers University of Technology in Sweden at a freestream velocity of 40 m/sec, corresponding to a unit Reynolds number of approximately 2.68×10^6/m (0.816×10^6/ft). The water surface was approximated by a plane at the load waterline, as shown in Fig. 6, and in this way the effects of waves were ignored, i.e., the Froude number was zero. This plane was represented in the wind tunnel as plane of symmetry by joining two models of the submerged part of the hull. At station 18, the boundary layer was tripped by cylindrical turbulence generators of 3 mm diam and 0.8 mm height, spaced by 9 mm.

The locations of boundary-layer traverses were selected on inviscid-flow-surface streamlines in order to facilitate comparison with boundary-layer calculations that proceed along such streamlines. The streamlines were known beforehand, and they were integrated from the output of the Douglas Neumann 3-D potential flow program.[7] Nine to twelve profiles were measured on each of seven streamlines between stations 16 and 1. Unfortunately, some of the edge streamline directions, as measured by the hot-wire probe, disagreed with the calculated inviscid flow directions by as much as two degrees in the forward half of the model and seven degrees in the aft half.

In order to check the accuracy of our boundary-layer method for this test, we have used "the small-cross flow method" described in Ref. 1. The calculations were started at the first measured station, No. 16, located at $x = 0.4$ m from the bow, i.e., at 20% of the total model length. The initial velocity profile on each streamline was generated by use of the procedure described previously. A comparison of calculated and experimental results for streamlines No. 3 and No. 5 are shown in Figs. 7 and 8. The boundary-layer parameters R_θ, H are calculated from

$$R_\theta = \theta_{11} u_s / \nu \qquad H = \delta_1^* / \theta_{11} \tag{28}$$

where u_s is the local streamwise edge velocity and

$$\theta_{11} = \int_0^\infty \frac{u}{u_s}\left(1 - \frac{u}{u_s}\right) dy \tag{29}$$

$$\delta_1^* = \int_0^\infty \left(1 - \frac{u}{u_s}\right) dy \tag{30}$$

For further comparison, see Ref. 8.

In conclusion, the method presented here for predicting the three-dimensional boundary layer is found to be in good agreement with the available experimental data as in the authors' previous studies.[1,2,9] The method accounts for both laminar and turbulent flows, and also for transitional flows in the rotating disk problem.

References

1 Cebeci, T., "Calculations of Three-Dimensional Boundary Layers. I. Swept Infinite Cylinders and Small Cross-Flow," *AIAA Journal*, Vol. 12, June 1974, pp. 779-786.

2 Bradshaw, P., "Calculation of Three-Dimensional Turbulent Boundary Layers," *Journal of Fluid Mechanics*, Vol. 46, Pt. 3, 1971, pp. 417-445.

3 Cebeci, T., "Calculation of Three-Dimensional Boundary Layers. II. Three-Dimensional Flows in Cartesian Coordinates," *AIAA Journal*, Vol. 13, Aug. 1975, pp. 1056-1064.

4 Vermeulen, A., Ph.D. thesis, Dept. of Engineering, Cambridge University (private communication).

5 Cebeci, T. and Smith, A.M.O., *Analysis of Turbulent Boundary Layers*, Academic Press, New York, 1974, p. 161.

6 Larsson, L., "Boundary Layers of Ships. III. An Experimental Investigation of the Turbulent Boundary Layer on a Ship Model," The Swedish State Shipbuilding Experimental Tank, Rept. 46, Sept. 1974.

7 Hess, J. L. and Smith, A.M.O., "Calculation of Nonlifting Potential Flow about Arbitrary Three-dimensional Bodies," Douglas Aircraft Co., Rept. E.S. 40622, March 1962.

8 Cebeci, T., Kaups, K., and Moser, A., "A General Method for Calculating Three-Dimensional Incompressible Laminar and Turbulent Boundary Layers," Douglas Aircraft Co., Rept. MDC J6867, April 1975.

9 Cebeci, T. and Abbott, D. E., "Boundary Layers on a Rotating Disk," *AIAA Journal*, Vol. 13, June 1975, pp. 829-832.